Continuum Mech. Thermodyn. (2016) 28:195–213
DOI 10.1007/s00161-015-0413-x

ORIGINAL ARTICLE

X.-L. Gao · G. Y. Zhang

A non-classical Kirchhoff plate model incorporating microstructure, surface energy and foundation effects

Received: 8 November 2014 / Accepted: 24 January 2015 / Published online: 21 February 2015

Abstract A new non-classical Kirchhoff plate model is developed using a modified couple stress theory, a surface elasticity theory and a two-parameter elastic foundation model. A variational formulation based on Hamilton's principle is employed, which leads to the simultaneous determination of the equations of motion and the complete boundary conditions and provides a unified treatment of the microstructure, surface energy and foundation effects. The new plate model contains a material length scale parameter to account for the microstructure effect, three surface elastic constants to describe the surface energy effect, and two foundation moduli to represent the foundation effect. The current non-classical plate model reduces to its classical elasticity-based counterpart when the microstructure, surface energy and foundation effects are all suppressed. In addition, the newly developed plate model includes the models considering the microstructure dependence or the surface energy effect or the foundation influence alone as special cases and recovers the Bernoulli–Euler beam model incorporating the microstructure, surface energy and foundation effects. To illustrate the new model, the static bending and free vibration problems of a simply supported rectangular plate are analytically solved by directly applying the general formulas derived. For the static bending problem, the numerical results reveal that the deflection of the simply supported plate with or without the elastic foundation predicted by the current model is smaller than that predicted by the classical model. Also, it is observed that the difference in the deflection predicted by the new and classical plate models is very large when the plate thickness is sufficiently small, but it is diminishing with the increase of the plate thickness. For the free vibration problem, it is found that the natural frequency predicted by the new plate model with or without the elastic foundation is higher than that predicted by the classical plate model, and the difference is significant for very thin plates. These predicted trends of the size effect at the micron scale agree with those observed experimentally. In addition, it is shown both analytically and numerically that the presence of the elastic foundation reduces the plate deflection and increases the plate natural frequency, as expected.

Keywords Kirchhoff plate · Size effect · Couple stress theory · Surface elasticity · Hamilton's principle · Winkler foundation · Pasternak foundation · Plate theory · Free vibration · Natural frequency

1 Introduction

Thin beams and plates widely used in MEMS and NEMS often exhibit microstructure- and surface energy-dependent size effects [23,32,33]. Classical continuum mechanics cannot be used to interpret such size effects

This paper is dedicated to Professor David J. Steigmann with deep gratitude.

Communicated by Victor Eremeyev, Peter Schiavone and Francesco dell'Isola.

X.-L. Gao (✉) · G. Y. Zhang
Department of Mechanical Engineering, Southern Methodist University, P. O. Box 750337, Dallas, TX 75275-0337, USA
E-mail: xlgao@smu.edu
Tel.: +1-214-768-1378

because of a lack of any material length scale parameter. Hence, models based on higher-order (non-classical) continuum theories that contain microstructure-dependent material parameters and can account for surface energy effects need to be developed.

In higher-order continuum mechanics theories, either a continuum embedded with microstructures or a non-local medium including long-range material interactions is employed (e.g., [31]). Strain gradient elasticity theories (e.g., [9,19,35]) make use of the former, whereas non-local elasticity theories (e.g., [5,6,20]) utilize the latter.

Several higher-order elasticity theories have been applied to develop non-classical plate models. Lazopoulos [21] provided a non-classical von Karman plate model based on a simplified strain gradient elasticity theory (SSGET) (e.g., [12,14]). This SSGET, which contains only one material length scale parameter, was also employed in [36,37] to derive non-classical equations of motion for Kirchhoff plates of strain gradient materials. By using a constitutive relation in non-local elasticity suggested in [5], Lu et al. [26] proposed a Kirchhoff plate model and a Mindlin plate model without using a variational formulation. Based on a modified couple stress theory that involves one additional material length scale parameter [39,53], three Kirchhoff plate models were suggested in [1,18,51], respectively. Recently, three new models for Mindlin plates and third-order shear deformation plates have been developed in [8,30,57] by using the modified couple stress theory and Hamilton's principle.

On the other hand, for solids with a large surface layer to bulk volume ratio, surface effects, which cannot be described using classical elasticity, become important (e.g., [33]). Such surface effects can be interpreted using a surface elasticity theory, in which the surface of a solid, where the atom arrangements and material properties differ from those in the bulk (e.g., [4]), is regarded as a membrane or film with a negligible thickness (e.g., [48,49]).

The surface elasticity theory (e.g., [15,16]) has been used to analyze thin plates involving surface effects. For example, Miller and Shenoy [33] developed a model to describe the size dependency of the effective stiffness of a nano-sized structural element (a bar, beam or plate). Lim and He [23] presented a geometrically nonlinear plate model for nano-scale films based on the Kirchhoff hypothesis and the von Karman strains. Lu et al. [25] constructed a size-dependent thin plate model by including the normal stress on and inside the surface of the bulk substrate. Lü et al. [27] developed a nonlinear plate model for functionally graded films using the Kirchhoff kinematic relations and the von Karman nonlinear strains for the bulk material. Wang and Wang [52] provided a model for nonlinear free vibrations of a Kirchhoff plate and a Mindlin plate using the von Karman strains.

However, very few models have been developed for thin plates by considering both the microstructure and surface energy effects. One non-classical model for Kirchhoff thin plates was provided in [22] by employing a strain gradient elasticity theory that contains two additional length scale parameters—one related to the bulk strain energy and the other linked to the surface energy. Another non-classical Kirchhoff plate model, which is based on a modified couple stress theory and a surface elasticity theory, was presented in [44] without using a variational formulation. The elastic foundation effect was not considered in either of these two studies.

The objective of the current paper is to develop a non-classical model for a Kirchhoff plate resting on a two-parameter elastic foundation characterized by the Winkler and Pasternak foundation moduli using the modified couple stress theory [39,53], the surface elasticity theory [15,16] and Hamilton's principle. This variational formulation leads to the simultaneous determination of the equations of motion and complete boundary conditions and provides a unified treatment of the microstructure, surface energy and foundation effects.

The rest of the paper is organized as follows. In Sect. 2, a new non-classical model for a Kirchhoff plate on a two-parameter elastic foundation is developed using a variational formulation based on Hamilton's principle. The newly obtained Kirchhoff plate model includes the models incorporating the microstructure dependence or the surface energy effect or the elastic foundation influence alone as special cases and recovers the model for Bernoulli–Euler beams based on the same modified couple stress theory and surface elasticity theory. Also, the new plate model reduces to its classical elasticity-based counterpart when the microstructure, surface energy and foundation effects are all suppressed. In Sect. 3, static bending and free vibration problems of a simply supported rectangular plate are analytically solved by directly applying the new model. The numerical results are also presented there to quantitatively show the differences between the current non-classical Kirchhoff plate model and its classical counterpart. The paper concludes in Sect. 4 with a summary.

2 Formulation

The Kirchhoff plate theory, also known as the classical plate theory, is the simplest theory for analyzing plates. It can be viewed as an extension of the Bernoulli–Euler beam theory to a two-dimensional plate theory.

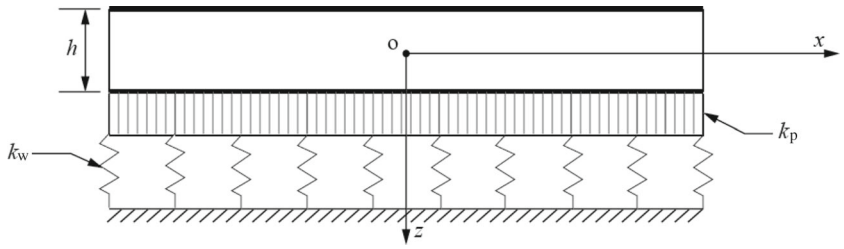

Fig. 1 Plate on a two-parameter elastic foundation

This classical plate theory has been generalized to include piezoelectric effects, leading to a piezo-electro-mechanical Kirchhoff–Love plate theory [2].

Consider a Kirchhoff plate resting on an elastic foundation that can be characterized by a two-parameter model including the Winkler foundation modulus k_w to represent the spring elements and the Pasternak foundation modulus k_p to describe the shear layer which is incompressible and deforms in transverse shear only (e.g., [43,54]), as schematically shown in Fig. 1. The effect of this two-parameter elastic foundation on the plate deformation can be equivalently represented as a vertical body force q (in N/m^2) given by [43]:

$$q(x, y, t) = k_w w(x, y, t) - k_p \nabla^2 w(x, y, t), \tag{1}$$

where ∇^2 is the Laplacian, and w is the displacement of point $(x,\ y,\ 0)$ on the mid-plane of the plate at time t.

By using the Cartesian coordinate system $(x,\ y,\ z)$ shown in Fig. 2, the displacement field in a Kirchhoff plate of uniform thickness h can be written as (e.g., [41])

$$u_1 = u(x, y, t) - z\frac{\partial w}{\partial x}, \quad u_2 = v(x, y, t) - z\frac{\partial w}{\partial y}, \quad u_3 = w(x, y, t), \tag{2a-c}$$

where u_1, u_2 and u_3 are, respectively, the x-, y- and z-components of the displacement vector $\boldsymbol{u}$ of a point $(x,\ y,\ z)$ in the plate at time t, and u, v and w are, respectively, the x-, y- and z-components of the displacement vector of the corresponding point $(x,\ y,\ 0)$ on the plate mid-plane at time t. Note that the subscripts 1, 2, 3 (rather than x, y, z) are employed in Eqs. (2a-c) to facilitate the use of the index notation in the variational formulation presented below.

In Fig. 2, S^+ and S^- denote, respectively, the lower and upper surface layers (with zero thickness) of the Kirchhoff plate. These two surface layers are taken to be perfectly bonded to the bulk plate material at $z = \pm h/2$, respectively. The bulk material satisfies the modified couple stress theory [39,53], while the surface layers have distinct material properties and are governed by the surface elasticity theory [15,16].

According to the modified couple stress theory [39,53], the constitutive equations for an isotropic linear elastic material read

$$\sigma_{ij} = \lambda\varepsilon_{kk}\delta_{ij} + 2\mu\varepsilon_{ij}, \tag{3}$$

$$m_{ij} = 2l^2\mu\chi_{ij}, \tag{4}$$

where σ_{ij} are the components of the Cauchy stress tensor, m_{ij} are the components of the deviatoric part of the couple stress tensor, δ_{ij} is the Kronecker delta, λ and μ are the Lamé constants in classical elasticity, l is a material length scale parameter measuring the couple stress effect (e.g., [34,38]), and ε_{ij} and χ_{ij} are, respectively, the components of the infinitesimal strain tensor and the symmetric curvature tensor defined by

$$\varepsilon_{ij} = \frac{1}{2}\left(u_{i,j} + u_{j,i}\right), \tag{5}$$

$$\chi_{ij} = \frac{1}{2}\left(\theta_{i,j} + \theta_{j,i}\right), \tag{6}$$

with u_i being the displacement components and θ_i being the components of the rotation vector defined as

$$\theta_i = \frac{1}{2}\varepsilon_{ijk}u_{k,j}. \tag{7}$$

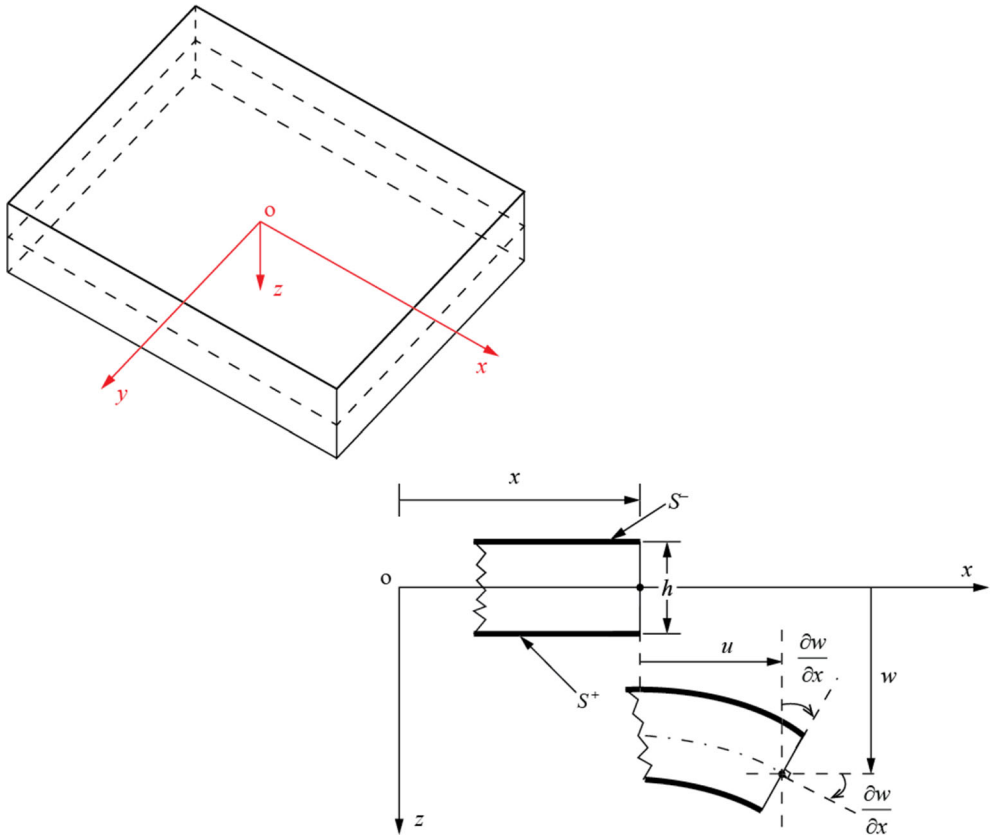

Fig. 2 Plate configuration and coordinate system

According to the surface elasticity theory (e.g., [15,16,48,49]), the surface layer of a bulk elastic material satisfies distinct constitutive equations involving surface elastic constants. The governing equations for the surface layer of zero thickness are given by (e.g., [16,42,56,58]):

$$\sigma_{ij}n_j = \tau_{i\alpha,\alpha}, \quad \sigma_{ij}n_i n_j = \tau_{\alpha\beta}\kappa_{\alpha\beta}, \tag{8a,b}$$

where $\kappa_{\alpha\beta}$ are the components of the surface curvature tensor, n_i are the components of the outward-pointing unit normal $\mathbf{n}(= n_i\mathbf{e}_i)$ to the surface, and $\tau_{\alpha\beta}$ are the in-plane components of the surface stress tensor expressed as [15,16]

$$\tau_{\alpha\beta} = \left[\tau_0 + (\lambda_0 + \tau_0)u_{\gamma,\gamma}\right]\delta_{\alpha\beta} + \mu_0\left(u_{\alpha,\beta} + u_{\beta,\alpha}\right) - \tau_0 u_{\beta,\alpha}, \tag{9}$$

where μ_0 and λ_0 are the surface elastic constants, and τ_0 is the residual surface stress (i.e., the surface stress at zero strain). These three constants μ_0, λ_0 and τ_0 can be determined from atomistic simulations (e.g., [33,45]) or experimental measurements (e.g., [17,55]). Clearly, Eq. (9) shows that $\tau_{\alpha\beta}$ is not symmetric.

The out-of-plane components of the surface stress tensor read [16]

$$\tau_{3\beta} = \tau_0 u_{3,\beta}. \tag{10}$$

Note that in Eqs. (3)–(10) and throughout the paper, the summation convention and standard index notation are used, with the Greek indices running from 1 to 2 and the Latin indices from 1 to 3 unless otherwise indicated.

It follows from Eqs. (2a-c) and (5)–(7) that in the bulk of the current Kirchhoff plate,

$$\varepsilon_{xx} = \frac{\partial u}{\partial x} - z\frac{\partial^2 w}{\partial x^2}, \quad \varepsilon_{xy} = \frac{1}{2}\left(\frac{\partial u}{\partial y} + \frac{\partial v}{\partial x} - 2z\frac{\partial^2 w}{\partial x \partial y}\right), \quad \varepsilon_{yy} = \frac{\partial v}{\partial y} - z\frac{\partial^2 w}{\partial y^2}, \quad \varepsilon_{xz} = \varepsilon_{yz} = \varepsilon_{zz} = 0, \tag{11}$$

$$\theta_1 = \frac{\partial w}{\partial y}, \quad \theta_2 = -\frac{\partial w}{\partial x}, \quad \theta_3 = \frac{1}{2}\left(\frac{\partial v}{\partial x} - \frac{\partial u}{\partial y}\right), \tag{12}$$

$$\chi_{xx}=\frac{\partial^2 w}{\partial x\partial y},\quad \chi_{xy}=\frac{1}{2}\left(\frac{\partial^2 w}{\partial y^2}-\frac{\partial^2 w}{\partial x^2}\right),\quad \chi_{yy}=-\frac{\partial^2 w}{\partial x\partial y},$$
$$\chi_{xz}=\frac{1}{4}\left(\frac{\partial^2 v}{\partial x^2}-\frac{\partial^2 u}{\partial x\partial y}\right),\quad \chi_{yz}=\frac{1}{4}\left(\frac{\partial^2 v}{\partial x\partial y}-\frac{\partial^2 u}{\partial y^2}\right),\quad \chi_{zz}=0. \tag{13}$$

The total strain energy in the elastically deformed Kirchhoff plate is given by

$$U_T=U_B+U_S+U_F=\frac{1}{2}\int_\Omega\left(\sigma_{ij}\varepsilon_{ij}+m_{ij}\chi_{ij}\right)\mathrm{d}V+\frac{1}{2}\int_{S^+}\tau_{\alpha\beta}\varepsilon_{\alpha\beta}\mathrm{d}A+\frac{1}{2}\int_{S^-}\tau_{\alpha\beta}\varepsilon_{\alpha\beta}\mathrm{d}A$$
$$+\frac{1}{2}\int_R k_{\mathrm{w}}w^2\mathrm{d}A+\frac{1}{2}\int_R k_{\mathrm{p}}\left(\frac{\partial w}{\partial x}\right)^2\mathrm{d}A+\frac{1}{2}\int_R k_{\mathrm{p}}\left(\frac{\partial w}{\partial y}\right)^2\mathrm{d}A, \tag{14}$$

where Ω is the region occupied by the plate, S^- and S^+ represent, respectively, the top and bottom surface layers of the plate (see Fig. 2), R denotes the area occupied by the mid-plane of the plate, $\mathrm{d}V$ is the volume element, and $\mathrm{d}A$ is the area element. In Eq. (14), U_B is the strain energy in the bulk of the plate, which is governed by the modified couple stress theory, U_S is the strain energy in the surface layers S^- and S^+ satisfying the surface elasticity theory, and U_F is the strain energy representing the effect of the two-parameter elastic foundation. Note that only the first part of U_B is considered in the classical Kirchhoff plate theory as the total strain energy (i.e., $U_T^C=\frac{1}{2}\int_\Omega\sigma_{ij}\varepsilon_{ij}\mathrm{d}V$) in the plate.

From Eqs. (9)–(14), the first variation of the total strain energy in the plate on the time interval $[0,\,T]$ can be obtained as

$$\delta\int_0^T U_T\mathrm{d}t=\int_0^T\int_\Omega\left(\sigma_{ij}\delta\varepsilon_{ij}+m_{ij}\delta\chi_{ij}\right)\mathrm{d}V\mathrm{d}t+\int_0^T\int_{S^+}\left(\tau_{\alpha\beta}^+-\frac{1}{2}\tau_0\delta_{\alpha\beta}\right)\delta\varepsilon_{\alpha\beta}^+\mathrm{d}A\mathrm{d}t$$
$$+\int_0^T\int_{S^-}\left(\tau_{\alpha\beta}^--\frac{1}{2}\tau_0\delta_{\alpha\beta}\right)\delta\varepsilon_{\alpha\beta}^-\mathrm{d}A\mathrm{d}t+\int_0^T\int_R k_{\mathrm{w}}w\delta w\mathrm{d}A\mathrm{d}t$$
$$-\int_0^T\int_R k_{\mathrm{p}}\left(\frac{\partial^2 w}{\partial x^2}+\frac{\partial^2 w}{\partial y^2}\right)\delta w\mathrm{d}A\mathrm{d}t$$
$$+\int_0^T\oint_{\partial R}k_{\mathrm{p}}\left(\frac{\partial w}{\partial x}n_x+\frac{\partial w}{\partial y}n_y\right)\delta w\mathrm{d}s\mathrm{d}t, \tag{15}$$

where ∂R is the boundary curve enclosing the area R, $\mathrm{d}s$ is the differential element of arc length along ∂R, and $\tau_{\alpha\beta}^+$ and $\tau_{\alpha\beta}^-$ represent, respectively, the surface stress components on the plate bottom (S^+) and top (S^-) surfaces. In reaching Eq. (15), use has been made of Green's theorem and the fact that $\tau_{\alpha\beta}$ is non-symmetric. This fact has been overlooked in other variational studies employing the surface elasticity theory [15,16].

Note that the volume integral of a sufficiently smooth function $D(x,\,y,\,z,\,t)$ over the region Ω occupied by a uniform-thickness plate can be represented by

$$\int_\Omega D(x,\,y,\,z,\,t)\mathrm{d}V=\int_R\int_{-h/2}^{h/2}D(x,\,y,\,z,\,t)\mathrm{d}z\mathrm{d}A, \tag{16}$$

where h is the plate thickness, and R is the plate mid-plane area.

Using Eqs. (11), (13) and (16) in (15) gives, with the help of Green's theorem,

$$\delta\int_0^T U_{\mathrm{T}}\mathrm{d}t=-\int_0^T\int_R\left\{\left[N_{xx,x}+N_{xy,y}+\frac{1}{2}\left(Y_{xz,xy}+Y_{yz,yy}\right)+\tau_{xx,x}^++\tau_{xx,x}^-+\frac{1}{2}\left(\tau_{xy,y}^++\tau_{xy,y}^-\right)\right.\right.$$
$$\left.+\frac{1}{2}\left(\tau_{yx,y}^++\tau_{yx,y}^-\right)\right]\delta u+\left[N_{yy,y}+N_{xy,x}-\frac{1}{2}\left(Y_{xz,xx}+Y_{yz,xy}\right)+\tau_{yy,y}^++\tau_{yy,y}^-+\frac{1}{2}\left(\tau_{xy,x}^++\tau_{xy,x}^-\right)\right.$$
$$\left.+\frac{1}{2}\left(\tau_{yx,x}^++\tau_{yx,x}^-\right)\right]\delta v+\left[M_{xx,xx}+2M_{xy,xy}+M_{yy,yy}-Y_{xx,xy}+Y_{xy,xx}-Y_{xy,yy}+Y_{yy,xy}\right.$$
$$\left.\left.+\frac{h}{2}\left(\tau_{\alpha\beta}^+-\tau_{\alpha\beta}^-\right)_{,\alpha\beta}-k_{\mathrm{w}}w+k_{\mathrm{p}}\left(\frac{\partial^2 w}{\partial x^2}+\frac{\partial^2 w}{\partial y^2}\right)\right]\delta w\right\}\mathrm{d}A\mathrm{d}t+\frac{1}{2}\int_0^T\oint_{\partial R}\left\{\left[2N_{xx}n_x+2N_{xy}n_y\right.\right.$$

$$+\frac{1}{2}\left(Y_{xz,x}n_y + Y_{xz,y}n_x\right) + Y_{yz,y}n_y + 2\left(\tau_{xx}^{+} + \tau_{xx}^{-} - \tau_0\right)n_x + \left(\tau_{xy}^{+} + \tau_{xy}^{-} + \tau_{yx}^{+} + \tau_{yx}^{-}\right)n_y\Bigg]\delta u$$
$$+\Bigg[2N_{xy}n_x + 2N_{yy}n_y - Y_{xz,x}n_x - \frac{1}{2}\left(Y_{yz,x}n_y + Y_{yz,y}n_x\right) + 2\left(\tau_{yy}^{+} + \tau_{yy}^{-} - \tau_0\right)n_y$$
$$+\left(\tau_{xy}^{+} + \tau_{xy}^{-} + \tau_{yx}^{+} + \tau_{yx}^{-}\right)n_x\Bigg]\delta v + \Bigg[2\left(M_{xx,x} + M_{xy,y}\right)n_x + 2\left(M_{xy,x} + M_{yy,y}\right)n_y$$
$$-\frac{1}{2}\left(Y_{xx} - Y_{yy}\right)_{,x}n_y - \frac{1}{2}\left(Y_{xx} - Y_{yy}\right)_{,y}n_x - \left(Y_{xx,x} + Y_{xy,y}\right)n_y + Y_{xy,x}n_x - Y_{xy,y}n_y + \left(Y_{xy,x} + Y_{yy,y}\right)n_x$$
$$+h\left(\tau_{\alpha\beta,\beta}^{+} - \tau_{\alpha\beta,\beta}^{-}\right)n_\alpha + 2k_{\mathrm{p}}\left(\frac{\partial w}{\partial x}n_x + \frac{\partial w}{\partial y}n_y\right)\Bigg]\delta w - \Bigg[2M_{xx}n_x + 2M_{xy}n_y - \frac{1}{2}\left(Y_{xx} - 3Y_{yy}\right)n_y$$
$$+2Y_{xy}n_x + h\left(\tau_{xx}^{+} - \tau_{xx}^{-}\right)n_x + h\left(\tau_{xy}^{+} - \tau_{xy}^{-}\right)n_y\Bigg]\delta w_{,x} - \Bigg[2M_{xy}n_x + 2M_{yy}n_y - \frac{1}{2}\left(3Y_{xx} - Y_{yy}\right)n_x$$
$$-2Y_{xy}n_y + h\left(\tau_{yx}^{+} - \tau_{yx}^{-}\right)n_x + h\left(\tau_{yy}^{+} - \tau_{yy}^{-}\right)n_y\Bigg]\delta w_{,y} - \frac{1}{2}Y_{xz}n_y\delta u_{,x} - \left(\frac{1}{2}Y_{xz}n_x + Y_{yz}n_y\right)\delta u_{,y}$$
$$+\frac{1}{2}\left(2Y_{xz}n_x + Y_{yz}n_y\right)\delta v_{,x} + \frac{1}{2}Y_{yz}n_x\delta v_{,y}\Bigg\}\,\mathrm{d}s\mathrm{d}t, \tag{17}$$

where

$$N_{xx} \equiv \int_{-h/2}^{h/2}\sigma_{xx}\mathrm{d}z, \quad N_{yy} \equiv \int_{-h/2}^{h/2}\sigma_{yy}\mathrm{d}z, \quad N_{xy} \equiv \int_{-h/2}^{h/2}\sigma_{xy}\mathrm{d}z,$$
$$M_{xx} \equiv \int_{-h/2}^{h/2}\sigma_{xx}z\mathrm{d}z, \quad M_{yy} \equiv \int_{-h/2}^{h/2}\sigma_{yy}z\mathrm{d}z, \quad M_{xy} \equiv \int_{-h/2}^{h/2}\sigma_{xy}z\mathrm{d}z,$$
$$Y_{xx} \equiv \int_{-h/2}^{h/2}m_{xx}\mathrm{d}z, \quad Y_{yy} \equiv \int_{-h/2}^{h/2}m_{yy}\mathrm{d}z, \quad Y_{xy} \equiv \int_{-h/2}^{h/2}m_{xy}\mathrm{d}z, \quad Y_{xz} \equiv \int_{-h/2}^{h/2}m_{xz}\mathrm{d}z,$$
$$Y_{yz} \equiv \int_{-h/2}^{h/2}m_{yz}\mathrm{d}z \tag{18}$$

are the Cauchy stress and couple stress resultants through the plate thickness. Note that in reaching Eq. (17) use has been made of the relations $S^+ = R = S^-$, $\partial S^+ = \partial R = \partial S^-$ for the uniform-thickness plate under consideration in order to facilitate the integral evaluations.

The kinetic energy of the plate has the form (e.g., [8,30])

$$K = \frac{1}{2}\int_\Omega \rho\left[(\dot{u}_1)^2 + (\dot{u}_2)^2 + (\dot{u}_3)^2\right]\mathrm{d}V, \tag{19}$$

where ρ is the mass density of the plate material. Note that here and in the sequel the overhead "$\cdot$" and "$\cdot\cdot$" denote, respectively, the first and second time derivatives (e.g., $\dot{u}_1 = \partial u_1/\partial t$, $\ddot{u}_1 = \partial^2 u_1/\partial t^2$). It should be mentioned that the kinetic energy given in Eq. (19) is not tied to the surface stress components on S^+ and S^-, since in the current formulation the surface effect is described using the surface elasticity theory of Gurtin and Murdoch [15,16], in which the surface layer is regarded as a thin film of zero thickness and thus has no mass or kinetic energy. If the surface layer were to be treated to have its own mass density, elastic properties, and inertia, then a different surface elasticity theory would have to be used in order to account for the effects of surface mass density and inertia on the kinetic energy and its variations (e.g., [40]).

From Eqs. (2a-c), (16) and (19), the first variation of the kinetic energy, on the time interval $[0,\ T]$, can be obtained as

$$\delta\int_0^T K\,\mathrm{d}t = -\int_0^T\int_R (m_0\ddot{u}\delta u + m_0\ddot{v}\delta v + m_0\ddot{w}\delta w + m_2\ddot{w}_{,x}\delta w_{,x} + m_2\ddot{w}_{,y}\delta w_{,y})\mathrm{d}A\mathrm{d}t, \tag{20}$$

where

$$m_0 \equiv \int_{-h/2}^{h/2}\rho\mathrm{d}z = \rho h, \quad m_2 \equiv \int_{-h/2}^{h/2}\rho z^2\mathrm{d}z = \frac{\rho h^3}{12}. \tag{21}$$

In reaching Eq. (20), it has been assumed that the initial ($t = 0$) and final ($t = T$) configurations of the plate are prescribed so that the virtual displacements vanish at $t = 0$ and $t = T$. In addition, ρ is taken to be constant along the plate thickness and over the time interval $[0,\ T]$ such that $\dot{m}_0 = 0,\quad \dot{m}_2 = 0$.

From the general expression of the work done by external forces in the modified couple stress theory [39] and in the surface elasticity theory [15,16], the virtual work done by the forces applied on the current plate over the time interval $[0,\ T]$ can be written as

$$\delta\int_0^T W\mathrm{d}t = \int_0^T\int_R (\mathbf{f}\cdot\delta\mathbf{u} + \mathbf{c}\cdot\delta\boldsymbol{\theta})\,\mathrm{d}A\mathrm{d}t + \int_0^T\oint_{\partial R}\left(\bar{\mathbf{t}}\cdot\delta\mathbf{u} + \bar{\mathbf{s}}\cdot\delta\boldsymbol{\theta}\right)\mathrm{d}s\mathrm{d}t + \int_0^T\int_S \mathbf{t}^s\cdot\delta(u_3\mathbf{e}_3)\mathrm{d}A\mathrm{d}t, \quad (22)$$

where $\mathbf{f}$ and $\mathbf{c}$ are, respectively, the body force resultant (force per unit area), body couple resultant (moment per unit area) through the plate thickness acting in the area R (i.e., the plate mid-plane), $\bar{\mathbf{t}}$ and $\bar{\mathbf{s}}$ are, respectively, the Cauchy traction resultant (force per unit length) and the surface couple resultant (moment per unit length) through the plate thickness acting on ∂R (i.e., the boundary of R), S represents the top and bottom surfaces of the plate (with $S = S^+ \cup S^-$), and $\mathbf{t}^s$ is the surface traction that is related to the surface stress $\boldsymbol{\tau}$ through $\mathbf{t}^s = \nabla_s\cdot\boldsymbol{\tau} = \tau_{i\alpha,\alpha}\mathbf{e}_i$ (e.g., [3,16]). Note that the last term in the virtual work expression in Eq. (22) accounts for the contribution of the normal stress on the top and bottom plate surfaces $\sigma_{33}^{\pm}$ ($= \pm\tau_{3\alpha,\alpha}^{\pm}$ from the equilibrium equations in Eq. (8a)), which is neglected in the classical Kirchhoff plate theory that does not consider the surface energy effect.

Using Eqs. (2a-c), (8a) and (12) in Eq. (22) leads to, with the help of Green's theorem,

$$\begin{aligned}\delta\int_0^T W\mathrm{d}t = &\int_0^T\int_R\left[f_x\delta u + f_y\delta v + f_z\delta w + c_x\delta w_{,y} - c_y\delta w_{,x} + \frac{1}{2}c_z(\delta v_{,x} - \delta u_{,y})\right]\mathrm{d}A\mathrm{d}t\\ &+\int_0^T\oint_{\partial R}\left[\overline{t_x}\delta u + \overline{t_y}\delta v + \overline{t_z}\delta w - \overline{M_x}\delta w_{,x} - \overline{M_y}\delta w_{,y} + \overline{s_x}\delta w_{,y} - \overline{s_y}\delta w_{,x}\right.\\ &\left.+\frac{1}{2}\overline{s_z}(\delta v_{,x} - \delta u_{,y})\right]\mathrm{d}s\mathrm{d}t\\ &+\int_0^T\int_{S^+}\tau_{3\alpha,\alpha}^{+}\delta w\mathrm{d}A\mathrm{d}t + \int_0^T\int_{S^-}\tau_{3\alpha,\alpha}^{-}\delta w\mathrm{d}A\mathrm{d}t,\end{aligned} \quad (23)$$

where f_i, c_i, $\overline{t_i}$ and $\overline{s_i}$ ($i = x,\ y,\ z$) are, respectively, the components of $\mathbf{f}$, $\mathbf{c}$, $\bar{\mathbf{t}}$ and $\bar{\mathbf{s}}$, and $\overline{M_x}$ and $\overline{M_y}$ are, respectively, the applied moments per unit length about the y-axis and x-axis acting on ∂R. Note that the positive directions of $\overline{M_x}$ and $\overline{M_y}$ are, respectively, opposite to those of $\partial w/\partial x$ and $\partial w/\partial y$ (see Fig. 2).

According to Hamilton's principle (e.g., [8,28–30,41]),

$$\delta\int_0^T [K - (U_T - W)]\ \mathrm{d}t = 0. \quad (24)$$

Using Eqs. (17), (20) and (23) in Eq. (24) and applying the fundamental lemma of the calculus of variations (e.g., [11,46,47]) will result in, with the arbitrariness of δu, δv and δw and the relations $S^+ = R = S^-$, $\partial S^+ = \partial R = \partial S^-$ due to the uniform thickness of the plate,

$$\begin{aligned}&N_{xx,x} + N_{xy,y} + \frac{1}{2}\left(Y_{xz,xy} + Y_{yz,yy}\right) + \tau_{xx,x}^{+} + \tau_{xx,x}^{-} + \frac{1}{2}\left(\tau_{xy,y}^{+} + \tau_{xy,y}^{-}\right) + \frac{1}{2}\left(\tau_{yx,y}^{+} + \tau_{yx,y}^{-}\right)\\ &\quad + f_x + \frac{1}{2}c_{z,y} = m_0\ddot{u},\end{aligned} \quad (25a)$$

$$\begin{aligned}&N_{xy,x} + N_{yy,y} - \frac{1}{2}\left(Y_{xz,xx} + Y_{yz,xy}\right) + \tau_{yy,y}^{+} + \tau_{yy,y}^{-} + \frac{1}{2}\left(\tau_{xy,x}^{+} + \tau_{xy,x}^{-}\right) + \frac{1}{2}\left(\tau_{yx,x}^{+} + \tau_{yx,x}^{-}\right)\\ &\quad + f_y - \frac{1}{2}c_{z,x} = m_0\ddot{v},\end{aligned} \quad (25b)$$

$$\begin{aligned}&M_{xx,xx} + 2M_{xy,xy} + M_{yy,yy} - Y_{xx,xy} + Y_{xy,xx} - Y_{xy,yy} + Y_{yy,xy} - k_{\mathrm{w}}w + k_{\mathrm{p}}\left(\frac{\partial^2 w}{\partial x^2} + \frac{\partial^2 w}{\partial y^2}\right)\\ &\quad + \frac{h}{2}\left(\tau_{\alpha\beta}^{+} - \tau_{\alpha\beta}^{-}\right)_{,\alpha\beta} + \tau_{3\alpha,\alpha}^{+} + \tau_{3\alpha,\alpha}^{-} + f_z - c_{x,y} + c_{y,x} = m_0\ddot{w} - m_2\frac{\partial^2\ddot{w}}{\partial x^2} - m_2\frac{\partial^2\ddot{w}}{\partial y^2}\end{aligned} \quad (25c)$$

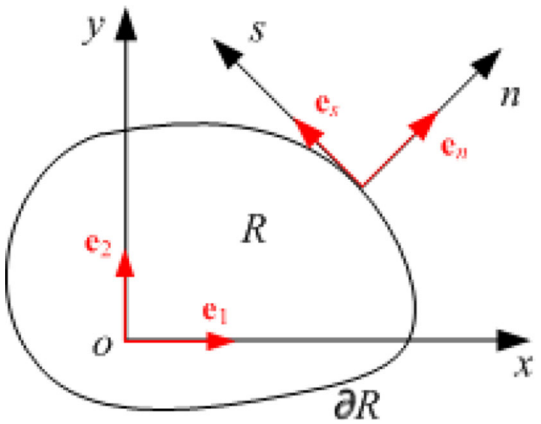

Fig. 3 Two coordinate systems

as the equations of motion of the Kirchhoff plate for any $(x,\ y) \in R$ and $t \in (0,\ T)$, and

$$
\begin{aligned}
&-\frac{1}{2}\int_0^T \oint_{\partial R} \Bigg\{ \Bigg[2N_{xx}n_x + 2N_{xy}n_y + \frac{1}{2}Y_{xz,x}n_y + \frac{1}{2}Y_{xz,y}n_x + Y_{yz,y}n_y + 2\left(\tau_{xx}^{+} + \tau_{xx}^{-} - \tau_0\right)n_x \\
&+ \left(\tau_{xy}^{+} + \tau_{xy}^{-} + \tau_{yx}^{+} + \tau_{yx}^{-}\right)n_y + c_z n_y - 2\overline{t_x} \Bigg] \delta u + \Bigg[2N_{xy}n_x + 2N_{yy}n_y - Y_{xz,x}n_x - \frac{1}{2}Y_{yz,x}n_y \\
&- \frac{1}{2}Y_{yz,y}n_x + \left(\tau_{xy}^{+} + \tau_{xy}^{-} + \tau_{yx}^{+} + \tau_{yx}^{-}\right)n_x + 2(\tau_{yy}^{+} + \tau_{yy}^{-} - \tau_0)n_y - c_z n_x - 2\overline{t_y} \Bigg] \delta v \\
&+ \Bigg[2(M_{xx,x} + M_{xy,y})n_x + 2(M_{xy,x} + M_{yy,y})n_y - \frac{1}{2}(Y_{xx} - Y_{yy})_{,x}n_y - \frac{1}{2}(Y_{xx} - Y_{yy})_{,y}n_x \\
&+ Y_{xy,x}n_x - Y_{xy,y}n_y + (Y_{xy,x} + Y_{yy,y})n_x - (Y_{xx,x} + Y_{xy,y})n_y + 2k_{\mathrm{p}}\left(\frac{\partial w}{\partial x}n_x + \frac{\partial w}{\partial y}n_y\right) \\
&+ h\left(\tau_{\alpha\beta,\beta}^{+} - \tau_{\alpha\beta,\beta}^{-}\right)n_\alpha - 2c_x n_y + 2c_y n_x - 2\overline{t_z} + 2m_2(\ddot{w}_{,x}n_x + \ddot{w}_{,y}n_y) \Bigg] \delta w - \Bigg[2M_{xx}n_x + 2M_{xy}n_y \\
&- \frac{1}{2}(Y_{xx} - 3Y_{yy})n_y + 2Y_{xy}n_x + h\left(\tau_{xx}^{+} - \tau_{xx}^{-}\right)n_x + h(\tau_{xy}^{+} - \tau_{xy}^{-})n_y - 2\overline{M_x} - 2\overline{s_y} \Bigg] \delta w_{,x} - \Bigg[2M_{xy}n_x \\
&+ 2M_{yy}n_y - \frac{1}{2}(3Y_{xx} - Y_{yy})n_x - 2Y_{xy}n_y + h\left(\tau_{yx}^{+} - \tau_{yx}^{-}\right)n_x + h\left(\tau_{yy}^{+} - \tau_{yy}^{-}\right)n_y - 2\overline{M_y} + 2\overline{s_x} \Bigg] \delta w_{,y} \\
&- \frac{1}{2}Y_{xz}n_y\delta u_{,x} - \left(\frac{1}{2}Y_{xz}n_x + Y_{yz}n_y - \overline{s_z}\right)\delta u_{,y} + \left(Y_{xz}n_x + \frac{1}{2}Y_{yz}n_y - \overline{s_z}\right)\delta v_{,x} + \frac{1}{2}Y_{yz}n_x\delta v_{,y} \Bigg\} \mathrm{d}s\mathrm{d}t \\
&= 0, \qquad (26)
\end{aligned}
$$

which can be further simplified to obtain the boundary conditions.

Note that the integrand of the line integral in Eq. (26) is expressed in terms of the Cartesian components of the resultants and displacements that are functions of the Cartesian coordinates $(x,\ y,\ z)$ with the unit base vectors $\{\mathbf{e}_1,\ \mathbf{e}_2,\ \mathbf{e}_3\}$. This is convenient for a rectangular plate whose edges are parallel to the x- and y-axes. However, for a more general case of a plate whose boundary is not aligned with the x- or y-axis, as shown in Fig. 3, it is more convenient to use a Cartesian coordinate system $(n,\ s,\ z)$ with the unit base vectors $\{\mathbf{e}_n,\ \mathbf{e}_s,\ \mathbf{e}_3\}$, where $\mathbf{e}_n\ (= n_x\mathbf{e_1} + n_y\mathbf{e_2})$ and $\mathbf{e}_s\ (= -n_y\mathbf{e_1} + n_x\mathbf{e_2})$ are, respectively, the unit normal and tangent vectors on the plate boundary ∂R.

It can be shown that the components in the coordinate system $(x,\ y,\ z)$ are related to those in the coordinate system $(n,\ s,\ z)$ through the following transformation expressions:

$$
\begin{aligned}
&\{u,\ v\}^T = [R_1]\{u_n,\ v_s\}^T, \quad \left\{w_{,x},\ w_{,y}\right\}^T = [R_1]\left\{w_{,n},\ w_{,s}\right\}^T, \\
&\left\{\overline{t_x},\ \overline{t_y}\right\}^T = [R_1]\left\{\overline{t_n},\ \overline{t_s}\right\}^T, \quad \left\{\overline{s_x},\ \overline{s_y}\right\}^T = [R_1]\left\{\overline{s_n},\ \overline{s_s}\right\}^T, \quad \left\{c_x,\ c_y\right\}^T = [R_1]\{c_n,\ c_s\}^T,
\end{aligned}
$$

$$
\begin{aligned}
&\left\{\overline{M_x},\ \overline{M_y}\right\}^T = [R_1]\left\{\overline{M_n},\ \overline{M_s}\right\}^T,\quad \left\{Y_{xz},\ Y_{yz}\right\}^T = [R_1]\left\{Y_{nz},\ Y_{sz}\right\}^T,\\
&\begin{bmatrix} N_{xx} & N_{xy} \\ N_{xy} & N_{yy} \end{bmatrix} = [R_1]\begin{bmatrix} N_{nn} & N_{ns} \\ N_{ns} & N_{ss} \end{bmatrix}[R_1]^T,\quad \begin{bmatrix} Y_{xx} & Y_{xy} \\ Y_{xy} & Y_{yy} \end{bmatrix} = [R_1]\begin{bmatrix} Y_{nn} & Y_{ns} \\ Y_{ns} & Y_{ss} \end{bmatrix}[R_1]^T,\\
&\begin{bmatrix} M_{xx} & M_{xy} \\ M_{xy} & M_{yy} \end{bmatrix} = [R_1]\begin{bmatrix} M_{nn} & M_{ns} \\ M_{ns} & M_{ss} \end{bmatrix}[R_1]^T,\quad \begin{bmatrix} Y_{xz,x} & Y_{xz,y} \\ Y_{yz,x} & Y_{yz,y} \end{bmatrix} = [R_1]\begin{bmatrix} Y_{nz,n} & Y_{nz,s} \\ Y_{sz,n} & Y_{sz,s} \end{bmatrix}[R_1]^T,\\
&\begin{bmatrix} \tau^{\pm}_{xx} & \tau^{\pm}_{xy} \\ \tau^{\pm}_{yx} & \tau^{\pm}_{yy} \end{bmatrix} = [R_1]\begin{bmatrix} \tau^{\pm}_{nn} & \tau^{\pm}_{ns} \\ \tau^{\pm}_{sn} & \tau^{\pm}_{ss} \end{bmatrix}[R_1]^T,\quad \begin{bmatrix} u_{,x} & u_{,y} \\ v_{,x} & v_{,y} \end{bmatrix} = [R_1]\begin{bmatrix} u_{n,n} & u_{n,s} \\ v_{s,n} & v_{s,s} \end{bmatrix}[R_1]^T,\\
&\left\{M_{xx,x},\ M_{xx,y}, M_{xy,x},\ M_{xy,y},\ M_{yy,x},\ M_{yy,y}\right\}^T = [R_3]\left\{M_{nn,n},\ M_{nn,s},\ M_{ns,n},\ M_{ns,s},\ M_{ss,n},\ M_{ss,s}\right\}^T,\\
&\left\{Y_{xx,x},\ Y_{xx,y},\ Y_{xy,x},\ Y_{xy,y},\ Y_{yy,x},\ Y_{yy,y}\right\}^T = [R_3]\left\{Y_{nn,n},\ Y_{nn,s},\ Y_{ns,n},\ Y_{ns,s},\ Y_{ss,n},\ Y_{ss,s}\right\}^T,\\
&\left\{\tau^{\pm}_{xx,x},\ \tau^{\pm}_{xy,y},\ \tau^{\pm}_{yx,x},\ \tau^{\pm}_{yy,y}\right\}^T = [R_4]\left\{\tau^{\pm}_{nn,n},\ \tau^{\pm}_{nn,s},\ \tau^{\pm}_{ns,n},\ \tau^{\pm}_{sn,n},\ \tau^{\pm}_{ns,s},\ \tau^{\pm}_{sn,s},\ \tau^{\pm}_{ss,n},\ \tau^{\pm}_{ss,s}\right\}^T,
\end{aligned}
\tag{27}
$$

where

$$
[R_1] \equiv \begin{bmatrix} n_x & -n_y \\ n_y & n_x \end{bmatrix},
$$

$$
[R_3] \equiv \begin{bmatrix}
n_x^3 & -n_x^2 n_y & -2n_x^2 n_y & 2n_x n_y^2 & n_x n_y^2 & -n_y^3 \\
n_x^2 n_y & n_x^3 & -2n_x n_y^2 & -2n_x^2 n_y & n_y^3 & n_x n_y^2 \\
n_x^2 n_y & -n_x n_y^2 & n_x^3 - n_x n_y^2 & -n_x^2 n_y + n_y^3 & -n_x^2 n_y & n_x n_y^2 \\
n_x n_y^2 & n_x^2 n_y & n_x^2 n_y - n_y^3 & n_x^3 - n_x n_y^2 & -n_x n_y^2 & -n_x^2 n_y \\
n_x n_y^2 & -n_y^3 & 2n_x^2 n_y & -2n_x n_y^2 & n_x^3 & -n_x^2 n_y \\
n_y^3 & n_x n_y^2 & 2n_x n_y^2 & 2n_x^2 n_y & n_x^2 n_y & n_x^3
\end{bmatrix},
$$

$$
[R_4] \equiv \begin{bmatrix}
n_x^3 & -n_x^2 n_y & -n_x^2 n_y & -n_x^2 n_y & n_x n_y^2 & n_x n_y^2 & n_x n_y^2 & -n_y^3 \\
n_x n_y^2 & n_x^2 n_y & n_x^2 n_y & -n_y^3 & n_x^3 & -n_x n_y^2 & -n_x n_y^2 & -n_x^2 n_y \\
n_x^2 n_y & -n_x n_y^2 & -n_x n_y^2 & n_x^3 & n_y^3 & -n_x^2 n_y & -n_x^2 n_y & n_x n_y^2 \\
n_y^3 & n_x n_y^2 & n_x n_y^2 & n_x n_y^2 & n_x^2 n_y & n_x^2 n_y & n_x^2 n_y & n_x^3
\end{bmatrix},
$$

(28a-c)

with $n_x^2 + n_y^2 = 1$.

Using Eqs. (27) and (28a-c) in Eq. (26) yields, after some lengthy algebra,

$$
\begin{aligned}
&\int_0^T \oint_{\partial R} \Big\{ 2\left(N_{nn} + \frac{1}{4}Y_{nz,s} + \tau^+_{nn} + \tau^-_{nn} - \tau_0 - \overline{t_n}\right)\delta u_n - \Big(-2N_{ns} + Y_{nz,n} + \frac{1}{2}Y_{sz,s} - \tau^+_{ns} - \tau^-_{ns} \\
&-\tau^+_{sn} - \tau^-_{sn} + c_z + 2\overline{t_s}\Big)\delta v_s + \Big[2M_{nn,n} + 2M_{ns,s} + h\left(\tau^+_{nn,n} - \tau^-_{nn,n} + \tau^+_{ns,s} - \tau^-_{ns,s}\right) - \frac{1}{2}Y_{nn,s} + 2Y_{ns,n} \\
&+\frac{3}{2}Y_{ss,s} + 2c_s - 2\overline{t_z} + 2m_2\ddot{w}_{,n} + 2k_{\mathrm{p}}w_{,n}\Big]\delta w + \left(-2Y_{ns} - 2M_{nn} - h\tau^+_{nn} + h\tau^-_{nn} + 2\overline{M_n} + 2\overline{s_s}\right)\delta w_{,n} \\
&+\left(-2M_{ns} + \frac{3}{2}Y_{nn} - \frac{1}{2}Y_{ss} - h\tau^+_{sn} + h\tau^-_{sn} + 2\overline{M_s} - 2\overline{s_n}\right)\delta w_{,s} + \left(-\frac{1}{2}Y_{nz} + \overline{s_z}\right)\delta u_{n,s} \\
&+(Y_{nz} - \overline{s_z})\delta v_{s,n} + \frac{1}{2}Y_{sz}\delta v_{s,s}\Big\}\,\mathrm{d}s\mathrm{d}t = 0.
\end{aligned}
\tag{29}
$$

Note that on the closed boundary ∂R, the following identity:

$$
\oint_{\partial R} D\delta g_{,s}\mathrm{d}s = -\oint_{\partial R} D_{,s}\delta g\mathrm{d}s \tag{30}
$$

holds, where D, g are two smooth functions. Using Eq. (30) in Eq. (29) leads to

$$
\int_0^T \oint_{\partial R} \left(\widehat{N}_{nn}\delta u_n + \widehat{N}_{ss}\delta v_s + \widehat{N}_{zz}\delta w + \widehat{T}_z\delta w_{,n} + \widehat{T}_s\delta v_{s,n}\right)\mathrm{d}s\mathrm{d}t = 0, \tag{31}
$$

where

$$\begin{aligned}
\widehat{N}_{nn} &\equiv 2\left(N_{nn}+\frac{1}{2}Y_{nz,s}+\tau_{nn}^{+}+\tau_{nn}^{-}-\tau_0-\frac{1}{2}\overline{s_{z,s}}-\overline{t_n}\right),\\
\widehat{N}_{ss} &\equiv 2N_{ns}-Y_{nz,n}-Y_{sz,s}+\tau_{ns}^{+}+\tau_{ns}^{-}+\tau_{sn}^{+}+\tau_{sn}^{-}-c_z-2\overline{t_s},\\
\widehat{N}_{zz} &\equiv 2M_{nn,n}+4M_{ns,s}-2Y_{nn,s}+2Y_{ns,n}+2Y_{ss,s}+h\left(\tau_{nn,n}^{+}-\tau_{nn,n}^{-}+\tau_{ns,s}^{+}-\tau_{ns,s}^{-}\right.\\
&\quad\left.+\tau_{sn,s}^{+}-\tau_{sn,s}^{-}\right)+2c_s-2\overline{M_{s,s}}+2\overline{s_{n,s}}-2\overline{t_z}+2m_2\ddot{w}_{,n}+2k_{\mathrm{p}}w_{,n},\\
\widehat{T}_z &\equiv -2Y_{ns}-2M_{nn}-h\tau_{nn}^{+}+h\tau_{nn}^{-}+2\overline{M_n}+2\overline{s_s},\\
\widehat{T}_s &\equiv Y_{nz}-\overline{s_z}.
\end{aligned}\tag{32a-e}$$

The use of the fundamental lemma of the calculus of variations in Eq. (31) gives

$$\begin{aligned}
\widehat{N}_{nn}=0 \quad &\text{or} \quad u_n=\overline{u_n},\\
\widehat{N}_{ss}=0 \quad &\text{or} \quad v_s=\overline{v_s},\\
\widehat{N}_{zz}=0 \quad &\text{or} \quad w=\overline{w},\\
\widehat{T}_z=0 \quad &\text{or} \quad w_{,n}=\overline{w_{,n}},\\
\widehat{T}_s=0 \quad &\text{or} \quad v_{s,n}=\overline{v_{s,n}}
\end{aligned}\tag{33a–e}$$

as the boundary conditions for any $(x,\ y)\in\partial R$ and $t\in(0,\ T)$, where the overhead bar defines the prescribed value.

From Eqs. (3), (4), (11), (13) and (18), the Cauchy stress and couple stress resultants can be expressed in terms of u, v and w as

$$\begin{aligned}
N_{xx} &= h\left[(\lambda+2\mu)\frac{\partial u}{\partial x}+\lambda\frac{\partial v}{\partial y}\right],\\
N_{yy} &= h\left[(\lambda+2\mu)\frac{\partial v}{\partial y}+\lambda\frac{\partial u}{\partial x}\right],\\
N_{xy} &= \mu h\left(\frac{\partial u}{\partial y}+\frac{\partial v}{\partial x}\right),\\
M_{xx} &= -\frac{1}{12}h^3\left[(\lambda+2\mu)\frac{\partial^2 w}{\partial x^2}+\lambda\frac{\partial^2 w}{\partial y^2}\right],\\
M_{yy} &= -\frac{1}{12}h^3\left[(\lambda+2\mu)\frac{\partial^2 w}{\partial y^2}+\lambda\frac{\partial^2 w}{\partial x^2}\right],\\
M_{xy} &= -\frac{1}{6}\mu h^3\frac{\partial^2 w}{\partial x\partial y},\\
Y_{xx} &= 2\mu l^2 h\frac{\partial^2 w}{\partial x\partial y},\\
Y_{yy} &= -2\mu l^2 h\frac{\partial^2 w}{\partial x\partial y},\\
Y_{xy} &= \mu l^2 h\left(\frac{\partial^2 w}{\partial y^2}-\frac{\partial^2 w}{\partial x^2}\right),\\
Y_{xz} &= \frac{1}{2}\mu l^2 h\left(\frac{\partial^2 v}{\partial x^2}-\frac{\partial^2 u}{\partial x\partial y}\right),\\
Y_{yz} &= \frac{1}{2}\mu l^2 h\left(\frac{\partial^2 v}{\partial x\partial y}-\frac{\partial^2 u}{\partial y^2}\right).
\end{aligned}\tag{34a-k}$$

From Eqs. (9), (10) and (2a-c), it follows that the surface stress components are given by

$$\tau_{xx}^{\pm}=\tau_0+(\lambda_0+\tau_0)\left(\frac{\partial v}{\partial y}\mp\frac{h}{2}\frac{\partial^2 w}{\partial y^2}\right)+(\lambda_0+2\mu_0)\left(\frac{\partial u}{\partial x}\mp\frac{h}{2}\frac{\partial^2 w}{\partial x^2}\right),$$

$$\tau_{yy}^{\pm} = \tau_0 + (\lambda_0 + \tau_0)\left(\frac{\partial u}{\partial x} \mp \frac{h}{2}\frac{\partial^2 w}{\partial x^2}\right) + (\lambda_0 + 2\mu_0)\left(\frac{\partial v}{\partial y} \mp \frac{h}{2}\frac{\partial^2 w}{\partial y^2}\right),$$
$$\tau_{xy}^{\pm} = \mu_0\left(\frac{\partial u}{\partial y} + \frac{\partial v}{\partial x}\right) - \tau_0\frac{\partial v}{\partial x} \mp \frac{1}{2}(2\mu_0 - \tau_0)h\frac{\partial^2 w}{\partial x \partial y},$$
$$\tau_{yx}^{\pm} = \mu_0\left(\frac{\partial u}{\partial y} + \frac{\partial v}{\partial x}\right) - \tau_0\frac{\partial u}{\partial y} \mp \frac{1}{2}(2\mu_0 - \tau_0)h\frac{\partial^2 w}{\partial x \partial y},$$
$$\tau_{3x}^{+} = \tau_{3x}^{-} = \tau_0\frac{\partial w}{\partial x},$$
$$\tau_{3y}^{+} = \tau_{3y}^{-} = \tau_0\frac{\partial w}{\partial y}. \tag{35a-f}$$

Using Eqs. (34a-k) and (35a-f) in Eqs. (25a-c) then yields the equations of motion of the Kirchhoff plate in terms of u, v and w as

$$(\lambda + 2\mu)hu_{,xx} + \mu h u_{,yy} + (\lambda + \mu)h v_{,xy} + \frac{1}{4}\mu l^2 h(-u_{,xxyy} - u_{,yyyy} + v_{,xxxy} + v_{,xyyy})$$
$$+2(2\mu_0 + \lambda_0)u_{,xx} + (2\mu_0 - \tau_0)u_{,yy} + (2\mu_0 + 2\lambda_0 + \tau_0)v_{,xy} + f_x + \frac{1}{2}c_{z,y} = m_0\ddot{u}, \tag{36a}$$
$$(\lambda + 2\mu)hv_{,yy} + \mu h v_{,xx} + (\lambda + \mu)h u_{,xy} + \frac{1}{4}\mu l^2 h(u_{,xxxy} + u_{,xyyy} - v_{,xxxx} - v_{,xxyy})$$
$$+2(2\mu_0 + \lambda_0)v_{,yy} + (2\mu_0 - \tau_0)v_{,xx} + (2\mu_0 + 2\lambda_0 + \tau_0)u_{,xy} + f_y - \frac{1}{2}c_{z,x} = m_0\ddot{v}, \tag{36b}$$
$$-\left[\frac{1}{12}(\lambda + 2\mu)h^3 + \mu l^2 h + \frac{1}{2}(\lambda_0 + 2\mu_0)h^2\right](w_{,xxxx} + 2w_{,xxyy} + w_{,yyyy})$$
$$+(2\tau_0 + k_{\mathrm{p}})(w_{,xx} + w_{,yy}) - k_{\mathrm{w}}w + f_z - c_{x,y} + c_{y,x} = m_0\ddot{w} - m_2\frac{\partial^2 \ddot{w}}{\partial x^2} - m_2\frac{\partial^2 \ddot{w}}{\partial y^2}. \tag{36c}$$

The boundary-initial value problem for determining u, v and w is defined by the differential equations in Eqs. (36a–c), the boundary conditions in Eqs. (33a–e), and given initial conditions at $t = 0$ and $t = T$. It is seen from Eqs. (36a–c) that the in-plane displacements u and v are uncoupled with the out-of-plane displacement w and can therefore be obtained separately from solving Eqs. (36a, b) subject to prescribed boundary conditions of the form in Eqs. (33a, b, e) and suitable initial conditions.

When $l = 0$ and $c_i = 0$, Eqs. (36a–c) will reduce to the governing equations for the Kirchhoff plate in the absence of the microstructure (or couple stress) effect.

When $\lambda_0 = \mu_0 = \tau_0 = 0$, Eqs. (36a–c) will become the governing equations for the Kirchhoff plate without the surface energy effect.

When $l = 0$, $c_i = 0$, and $\lambda_0 = \mu_0 = \tau_0 = 0$, Eqs. (36a–c) will degenerate to the classical elasticity-based governing equations for the Kirchhoff plate resting on the two-parameter elastic foundation.

When $l = 0$, $c_i = 0$, $\lambda_0 = \mu_0 = \tau_0 = 0$, and $k_{\mathrm{w}} = k_{\mathrm{p}} = 0$, Eqs. (36a–c) reduce to

$$(\lambda + 2\mu)hu_{,xx} + \mu h u_{,yy} + (\lambda + \mu)h v_{,xy} + f_x = m_0\ddot{u}, \tag{37a}$$
$$(\lambda + 2\mu)hv_{,yy} + \mu h v_{,xx} + (\lambda + \mu)h u_{,xy} + f_y = m_0\ddot{v}, \tag{37b}$$
$$-\frac{1}{12}(\lambda + 2\mu)h^3(w_{,xxxx} + 2w_{,xxyy} + w_{,yyyy}) + f_z = m_0\ddot{w} - m_2\frac{\partial^2 \ddot{w}}{\partial x^2} - m_2\frac{\partial^2 \ddot{w}}{\partial y^2}, \tag{37c}$$

which are the governing equations for the Kirchhoff plate based on classical elasticity.

When $u = v = 0$, $w = w(x, t)$, $f_x = f_y = 0$, and $c_x = c_z = 0$, the Kirchhoff plate considered here becomes a Bernoulli–Euler beam with a unit width and a height h undergoing only bending deformations. For this case, Eqs. (36a–c) are simplified as

$$-\left[\frac{1}{12}(\lambda + 2\mu)h^3 + \mu l^2 h + \frac{1}{2}(\lambda_0 + 2\mu_0)h^2\right]w_{,xxxx} + (2\tau_0 + k_{\mathrm{p}})w_{,xx} - k_{\mathrm{w}}w + f_z + c_{y,x}$$
$$= m_0\ddot{w} - m_2\frac{\partial^2 \ddot{w}}{\partial x^2} \tag{38}$$

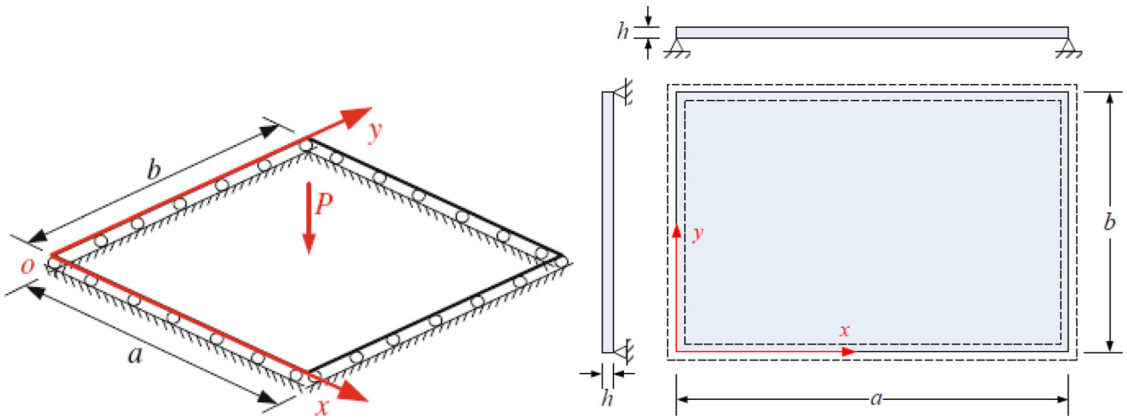

Fig. 4 Simply supported plate

for any $x \in (0,\ L)$ and $t \in (0,\ T)$, where L is the length of the beam (plate). When the elastic foundation is not present (i.e., $k_{\mathrm{w}} = k_{\mathrm{p}} = 0$), the governing equation in Eq. (38) reduces to that for the Bernoulli–Euler beam with a unit width and a height h without considering axial loading and the surface energy effect on the two side surfaces of the beam [7,13]. That is, the current Kirchhoff plate model recovers the non-classical Bernoulli–Euler beam model based on the same modified couple stress theory and surface elasticity theory. For static bending, $w = w(x)$, and Eq. (38) further reduces to the static equilibrium equation for a Bernoulli–Euler beam without the elastic foundation derived in [10].

3 Examples: static bending and free vibration of a simply supported plate

To demonstrate the new Kirchhoff model developed in Sect. 2, static bending and free vibration problems of a simply supported rectangular plate (see Fig. 4) are analytically solved herein by directly applying the new model.

In view of the general form of the boundary conditions (BCs) in Eqs. (33a–e), the BCs for this simply supported plate can be identified as

$$u_n = 0, \quad \widehat{N}_{ss} = 0, \quad w = 0, \quad \widehat{T}_z = 0, \quad \widehat{T}_s = 0 \tag{39}$$

for all $(x,\ y)$ on the boundaries $x = 0,\ a$ and $y = 0,\ b$. Also, the following applied traction resultants vanish on these boundaries:

$$\overline{s_s} = \overline{s_z} = 0, \quad \overline{M_n} = 0, \quad \overline{t_s} = 0. \tag{40}$$

For the boundaries $x = 0,\ a$, $n_y = 0$ and $n_x = -1$ (on $x = 0$) or $n_x = 1$ (on $x = a$), and Eq. (39) becomes, with the help of Eqs. (27), (28a), (32b, d, e) and (40),

$$\begin{aligned}
&u(0,\ y) = u(a,\ y) = 0,\\
&w(0,\ y) = w(a,\ y) = 0,\\
&N_{xy} - \frac{1}{2}Y_{xz,x} - \frac{1}{2}Y_{yz,y} + \frac{1}{2}\left(\tau_{xy}^{+} + \tau_{xy}^{-} + \tau_{yx}^{+} + \tau_{yx}^{-}\right) - \frac{1}{2}c_z = 0 \text{ on } x = 0 \text{ and } x = a,\\
&M_{xx} + Y_{xy} + \frac{h}{2}\left(\tau_{xx}^{+} - \tau_{xx}^{-}\right) = 0 \quad \text{on } x = 0 \text{ and } x = a,\\
&Y_{xz} = 0 \quad \text{on } x = 0 \text{ and } x = a.
\end{aligned} \tag{41a–e}$$

Using Eqs. (34c, d, i–k) and (35a, c, d) in Eqs. (41c–e) gives

$$\begin{aligned}
&\mu h(u_{,y} + v_{,x}) + \frac{1}{4}\mu l^2 h(u_{,xxy} - v_{,xxx}) + \frac{1}{4}\mu l^2 h(u_{,yyy} - v_{,xyy}) + (2\mu_0 - \tau_0)(u_{,y} + v_{,x}) - \frac{1}{2}c_z = 0,\\
&\mu l^2 h(-w_{,xx} + w_{,yy}) - \frac{1}{12}h^3[(\lambda + 2\mu)w_{,xx} + \lambda w_{,yy}] - \frac{1}{2}h^2(\lambda_0 + 2\mu_0)w_{,xx} - \frac{1}{2}h^2(\lambda_0 + \tau_0)w_{,yy} = 0,\\
&-u_{,xy} + v_{,xx} = 0
\end{aligned} \tag{42a–c}$$

on $x = 0$ and $x = a$.

For the boundaries $y = 0,\ b$, $n_x = 0$ and $n_y = -1$ (on $y = 0$) or $n_y = 1$ (on $y = b$), and Eq. (39) now becomes, with the help of Eqs. (27), (28a), (32b, d, e) and (40),

$$
\begin{aligned}
&v(x,0) = v(x,b) = 0,\\
&w(x,0) = w(x,b) = 0,\\
&-N_{xy} - \frac{1}{2}(Y_{xz,x} + Y_{yz,y}) - \frac{1}{2}(\tau_{xy}^{+} + \tau_{xy}^{-} + \tau_{yx}^{+} + \tau_{yx}^{-}) - \frac{1}{2}c_z = 0 \quad \text{on } y = 0 \text{ and } y = b,\\
&M_{yy} - Y_{xy} + \frac{h}{2}(\tau_{yy}^{+} - \tau_{yy}^{-}) = 0 \quad \text{on } y = 0 \text{ and } y = b,\\
&Y_{yz} = 0 \quad \text{on } y = 0 \text{ and } y = b.
\end{aligned}
\tag{43a-e}
$$

Using Eqs. (34c, e, i–k) and (35b–d) in Eqs. (43c–e) results in

$$
\begin{aligned}
&\mu h(u_{,y} + v_{,x}) - \frac{1}{4}\mu l^2 h(u_{,yyy} - v_{,xyy}) - \frac{1}{4}\mu l^2 h(u_{,xxy} - v_{,xxx}) + (2\mu_0 - \tau_0)(u_{,y} + v_{,x}) + \frac{1}{2}c_z = 0,\\
&\mu l^2 h(w_{,xx} - w_{,yy}) - \frac{1}{12}h^3[\lambda w_{,xx} + (\lambda + 2\mu)w_{,yy}] - \frac{1}{2}h^2[(\lambda_0 + \tau_0)w_{,xx} + (\lambda_0 + 2\mu_0)w_{,yy}] = 0,\\
&u_{,yy} - v_{,xy} = 0
\end{aligned}
\tag{44a–c}
$$

on $y = 0$ and $y = b$.

3.1 Static bending

For static bending problems, u, v and w are independent of time t so that all of the time derivatives involved in Eqs. (36a–c) vanish.

The boundary value problem (BVP) for the static bending of the simply supported plate shown in Fig. 4 is defined by Eqs. (36a–c) and the boundary conditions in Eqs. (41a, b), (42a–c), (43a, b) and (44a–c), with $u = u(x, y)$, $v = v(x, y)$ and $w = w(x, y)$.

As mentioned in Sect. 2, the in-plane displacements u and v are uncoupled with w. They can be obtained from solving the BVP defined by Eqs. (36a), (36b), (41a), (42a, c), (43a) and (44a, c). For the current case with $f_x = f_y = 0$ and $c_z = 0$, the solution of this BVP gives $u = v = 0$ for any $(x, y) \in R$.

The out-of-plane displacement w can be obtained from solving the BVP defined by Eqs. (36c), (41b), (42b), (43b) and (44b).

Consider the following Fourier series solution for w:

$$
w = \sum_{m=1}^{\infty}\sum_{n=1}^{\infty} W_{mn} \sin\left(\frac{m\pi x}{a}\right) \sin\left(\frac{n\pi y}{b}\right), \tag{45}
$$

where W_{mn} is the Fourier coefficient to be determined for each pair of m and n. It can be readily shown that w in Eq. (45) satisfies the boundary conditions in Eqs. (41b), (42b) at $x = 0,\ a$ and in Eqs. (43b), (44b) at $y = 0,\ b$ for any W_{mn}.

The force $f_z(x, y)$ involved in Eq. (36c) can also be expanded in a Fourier series as

$$
f_z(x, y) = \sum_{m=1}^{\infty}\sum_{n=1}^{\infty} Q_{mn} \sin\left(\frac{m\pi x}{a}\right) \sin\left(\frac{n\pi y}{b}\right), \tag{46}
$$

where the Fourier coefficient Q_{mn} is given by

$$
Q_{mn} = \frac{4}{ab}\int_0^a \int_0^b f_z(x, y) \sin\left(\frac{m\pi x}{a}\right) \sin\left(\frac{n\pi y}{b}\right) \mathrm{d}x\mathrm{d}y. \tag{47}
$$

In the current case (see Fig. 4), $f_z(x, y) = P\delta(x - \frac{a}{2})\delta(y - \frac{b}{2})$, where $\delta(\cdot)$ is the Dirac delta function. Using this f_z in Eq. (47) yields

$$
Q_{mn} = \frac{4P}{ab} \sin\left(\frac{m\pi}{2}\right) \sin\left(\frac{n\pi}{2}\right). \tag{48}
$$

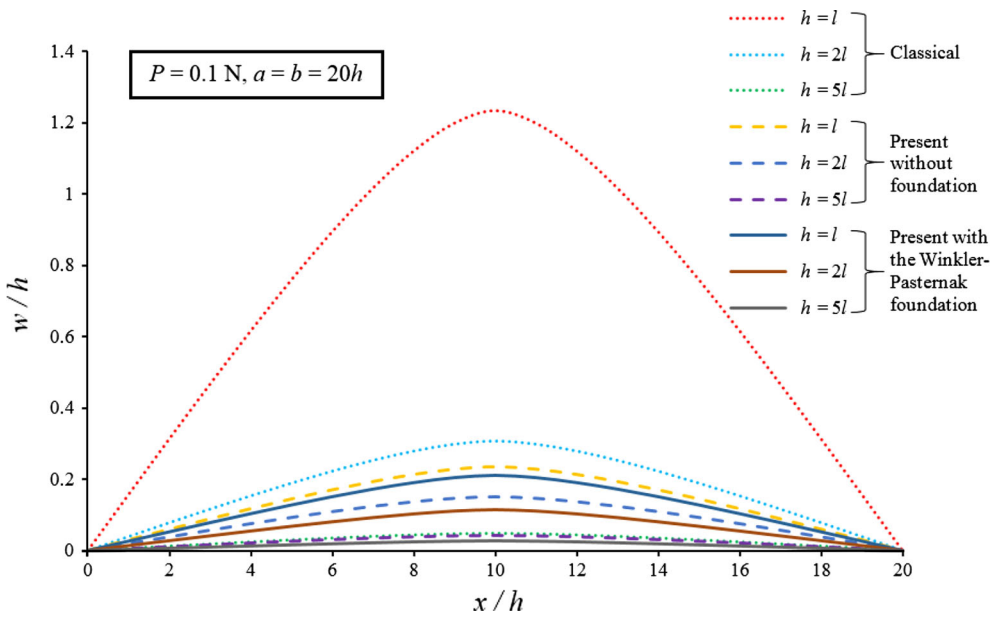

Fig. 5 Deflection of the simply supported Kirchhoff plate on $y = b/2$ with $\bar{K}_{\mathrm{w}} = 100$, $\bar{K}_{\mathrm{p}} = 10$

Using Eqs. (45) and (46) in Eq. (36c) results in, with $c_x = c_y = 0$,

$$W_{mn} = \frac{Q_{mn}}{\Delta} \tag{49}$$

where

$$\Delta \equiv \left[\frac{h^3}{12}(\lambda + 2\mu) + \mu l^2 h + \frac{h^2}{2}(\lambda_0 + 2\mu_0)\right]\left(\frac{m^2\pi^2}{a^2} + \frac{n^2\pi^2}{b^2}\right)^2 + (2\tau_0 + k_{\mathrm{p}})\left(\frac{m^2\pi^2}{a^2} + \frac{n^2\pi^2}{b^2}\right) + k_{\mathrm{w}}. \tag{50}$$

Substituting this W_{mn} into Eq. (45) will give the exact solution w based on the current non-classical Kirchhoff plate model for the simply supported plate subjected to the concentrated force at the center of the plate shown in Fig. 4.

Clearly, Eqs. (49) and (50) show that the incorporation of the microstructure effect (i.e., with $l \neq 0$) will always lead to increased plate stiffness (thus reduced deflections), while the inclusion of the surface energy effect (i.e., with any of $\{\mu_0, \lambda_0, \tau_0\}$ not being zero) can result in either increased or decreased plate stiffness, depending on the signs of $2\mu_0 + \lambda_0$ and τ_0. It is also seen from Eqs. (49) and (50) that the presence of the elastic foundation (i.e., with $k_{\mathrm{w}} > 0$ and/or $k_{\mathrm{p}} > 0$) will always lead to reduced plate deflection.

Figure 5 displays the variations of the plate deflection w along the line $y = b/2$ predicted by the current non-classical Kirchhoff plate model and by its classical elasticity-based counterpart. The numerical results predicted by the new model are directly obtained from Eqs. (45) and (48)–(50), while those by the classical model are computed using the same equations but with $l = 0$, $\lambda_0 = \mu_0 = \tau_0 = 0$, and $k_{\mathrm{w}} = k_{\mathrm{p}} = 0$. In generating the numerical results shown in Fig. 5, the shape of the plate is fixed by letting $a = b = 20h$, while the plate thickness h is varying. The plate material is taken to be aluminum with the following properties [10,24]: $E = 90\,\mathrm{GPa}$, $\nu = 0.23$, $l = 6.58\,\mu\mathrm{m}$ for the bulk properties, and $\mu_0 = -5.4251\,\mathrm{N/m}$, $\lambda_0 = 3.4939\,\mathrm{N/m}$, $\tau_0 = 0.5689\,\mathrm{N/m}$ for the surface layers, where Young's modulus E and Poisson's ratio ν are related to the Lamé constants λ and μ through (e.g., [50]):

$$\lambda = \frac{E\nu}{(1+\nu)(1-2\nu)}, \quad \mu = \frac{E}{2(1+\nu)}. \tag{51}$$

The foundation moduli are non-dimensionalized and taken to be $\bar{K}_{\mathrm{w}} = 100$, $\bar{K}_{\mathrm{p}} = 10$, where $\bar{K}_{\mathrm{w}} \equiv k_{\mathrm{w}}a^4/D$, $\bar{K}_{\mathrm{p}} \equiv k_{\mathrm{p}}a^2/D$, with $D = Eh^3/[12(1-\nu^2)]$ being the plate flexural rigidity. The number of terms

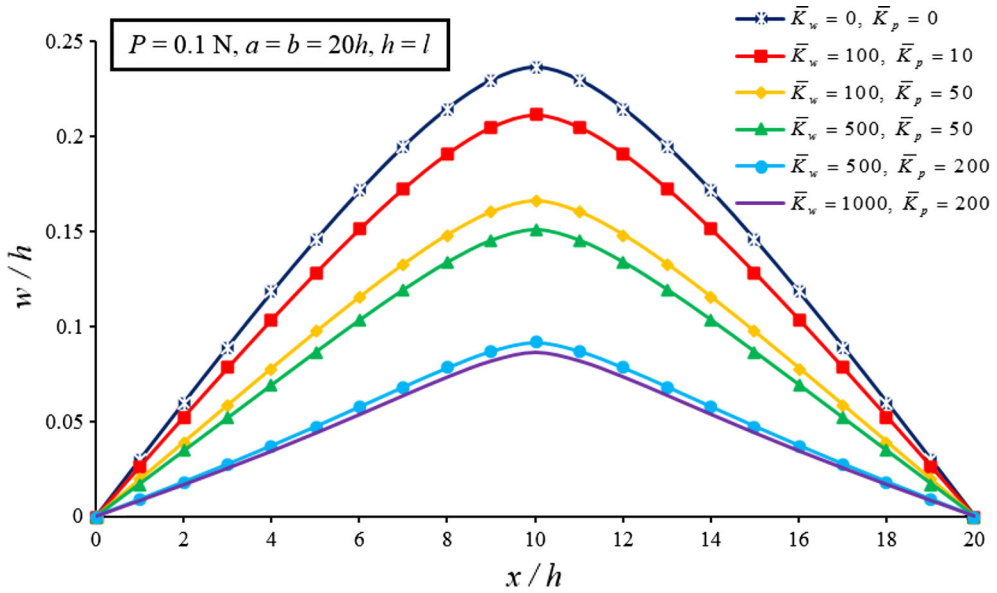

Fig. 6 Deflection of the plate with different values of k_w and k_p

included in Eq. (45) is controlled by adjusting m and n. The numerical results for the plate deflection w obtained with $m = 30$ and $n = 30$ are found to be the same as those computed with larger m and n values (up to $m = 90$, $n = 90$) to the fourth decimal place. This indicates that using $m = 30$, $n = 30$ in the expansion is sufficient for the convergent numerical solution of w displayed in Fig. 5.

From Fig. 5, it is clearly seen that the deflection w predicted by the current Kirchhoff model with or without the foundation is always lower than that predicted by the classical model in all cases considered. It also shows that the differences between the values predicted by the new model and the classical model are very large when the thickness of the plate h is small (with $h = l = 6.58\,\mu$m here), but the differences are diminishing when the thickness of the plate h becomes large (with $h = 5l = 32.9\,\mu$m here). This predicted size effect agrees with the general trend observed experimentally (e.g., [32]). In addition, it is observed from Fig. 5 that the presence of the elastic foundation does reduce the plate deflection, as expected (and noted earlier from Eqs. (49) and (50)). This is further shown in Fig. 6, where more cases with different values of k_w and k_p are compared, including the case without the foundation (as the top curve with $k_w = k_p = 0$). Note that the values of the other parameters are the same as those used in obtaining the numerical results shown in Fig. 5.

Both the microstructure and surface energy effects are included in the numerical results shown in Figs. 5 and 6. To illustrate the surface energy effect, additional numerical results are presented in Fig. 7 for the deflection of the simply supported plate shown in Fig. 4, which are obtained from Eqs. (45) and (48)–(50) by letting $l = 0$. For comparison purposes, the results predicted by the classical elasticity-based Kirchhoff plate model are also plotted in Fig. 7, which are computed using (45) and (48)–(50) with $l = 0$ and $\lambda_0 = \mu_0 = \tau_0 = 0$. The plate material in this case is taken to be iron with the following properties [16]: $E = 177.33$ GPa, $\nu = 0.27$ for the bulk, and $\mu_0 = 2.5$ N/m, $\lambda_0 = -8$ N/m, $\tau_0 = 1.7$ N/m for the surface layers. The cross-sectional shape is kept to be the same by letting $a = b = 20h$ (see Fig. 4) for all cases. In addition, the foundation moduli are set to be $k_w = k_p = 0$ to examine only the surface energy effect.

From Fig. 7, it is observed that the plate deflection predicted by the current model including the surface energy effect alone is always smaller than those predicted by the classical model in all cases considered here for the iron plate. Figure 7 also shows that the differences between the two sets of predicted values are significant only when the plate thickness h is very small, but they are diminishing as h increases. This indicates that the surface effect is important only when the plate is sufficiently thin.

3.2 Free vibration

For free vibration problems, the BVP for the simply supported plate shown in Fig. 4 is defined by Eqs. (36a–c), (41a, b), (42a–c), (43a, b) and (44a–c), with all external forces vanished (i.e., $f_x = f_y = f_z = 0$ and $c_x = c_y = c_z = 0$).

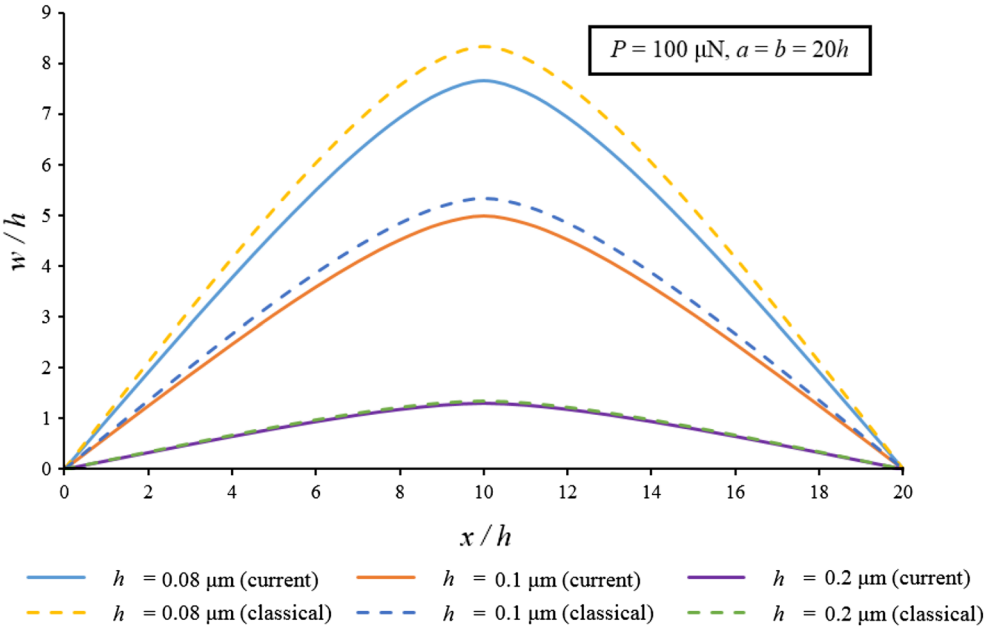

Fig. 7 Deflection of the simply supported plate predicted by the new model considering the surface energy effect alone (i.e., with $l = k_{\mathrm{w}} = k_{\mathrm{p}} = 0$) and by the classical model

For the current case with $f_x = f_y = 0$ and $c_z = 0$, Eqs. (36a, b), (41a), (42a, c), (43a) and (44a, c) give $u = u(x,\ y,\ t) = 0,\ v = v(x,\ y,\ t) = 0$ for any $(x,\ y) \in R$ and $t \in [0,\ T]$.

For $w = w(x,\ y,\ t)$, consider the following Fourier series expansion:

$$w(x,\ y,\ t) = \sum_{m=1}^{\infty}\sum_{n=1}^{\infty} W_{mn}^{V} \sin\left(\frac{m\pi x}{a}\right) \sin\left(\frac{n\pi y}{b}\right) e^{i\omega_n t}, \tag{52}$$

where ω_n is the nth natural frequency of vibration of the plate, W_{mn}^{V} is the Fourier coefficient, and i is the imaginary unit satisfying $i^2 = -1$. It can be readily shown that w in Eq. (52) satisfies the boundary conditions in Eqs. (41b), (42b), (43b) and (44b) for any t $[0,\ T]$.

Using Eq. (52) in Eq. (36c) gives, for a non-trivial solution with $W_{mn}^{V} \neq 0$,

$$\omega_n = \sqrt{\frac{k_{\mathrm{w}} + \left\{2\tau_0 + k_{\mathrm{p}} + \left[\frac{h^3}{12}(\lambda + 2\mu) + \mu l^2 h + \frac{h^2}{2}(\lambda_0 + 2\mu_0)\right]\left(\frac{m^2\pi^2}{a^2} + \frac{n^2\pi^2}{b^2}\right)\right\}\left(\frac{m^2\pi^2}{a^2} + \frac{n^2\pi^2}{b^2}\right)}{\rho h + \frac{1}{12}\rho h^3\left(\frac{m^2\pi^2}{a^2} + \frac{n^2\pi^2}{b^2}\right)}}, \tag{53}$$

where use has been made of Eq. (21). From Eq. (53), it is seen that the inclusion of the microstructure effect (with $l \neq 0$) and the presence of the foundation (with $k_{\mathrm{w}} > 0$ and/or $k_{\mathrm{p}} > 0$) will always lead to increased values of ω_n, while the incorporation of the surface energy effect may result in increased or decreased values of ω_n, depending on the signs of $\lambda_0 + 2\mu_0$ and τ_0.

Figure 8 shows the variation of the first natural frequency ω_1 obtained from Eq. (53) (with $m = 1,\ n = 1$) with the plate thickness predicted by the current Kirchhoff plate model and by the classical model. The results for the current plate model with the Winkler–Pasternak ($\bar{K}_{\mathrm{w}} = 1000,\ \bar{K}_{\mathrm{p}} = 100$) or Winkler ($\bar{K}_{\mathrm{w}} = 1000,\ k_{\mathrm{p}} = 0$) or no foundation ($k_{\mathrm{w}} = k_{\mathrm{p}} = 0$) shown in Fig. 8 are obtained from Eq. (53), while those for the classical plate model are computed from the same equation but with $l = 0,\ \lambda_0 = \mu_0 = \tau_0 = 0$, and $k_{\mathrm{w}} = k_{\mathrm{p}} = 0$. The material properties and geometry of the aluminum plate used here are the same as those employed earlier to obtain the numerical results displayed in Figs. 5 and 6. In addition, the density for the aluminum plate is taken to be $\rho = 2.7 \times 10^3$ kg/m^3, which is needed in Eq. (53).

From Fig. 8, it is clearly seen that the natural frequency predicted by the current model with or without the foundation is always higher than that predicted by the classical elasticity-based model. The difference between

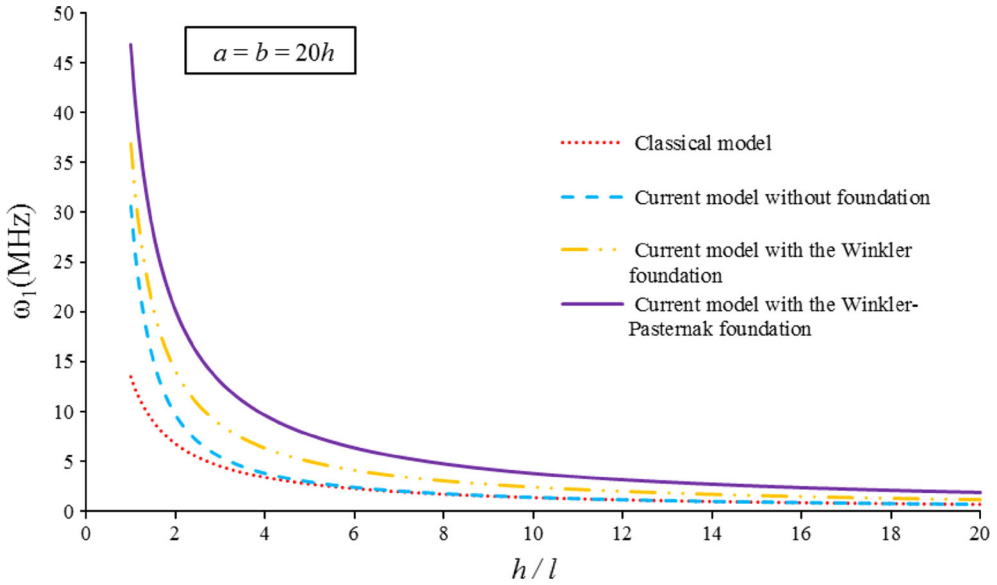

Fig. 8 Natural frequency varying with the plate thickness

the predictions by the current model (with the microstructure and surface energy effects) and the classical model is significant when the plate thickness h is very small (with $h < 2l = 13.16\,\mu\text{m}$ here if excluding the foundation effect). However, the difference is diminishing as h becomes large (with $h > 6l = 39.48\,\mu\text{m}$ here for the case with $k_{\text{w}} = k_{\text{p}} = 0$). This shows that the size effect on the natural frequency is important only when the plate thickness is very small. In addition, it is observed from Fig. 8 that the presence of the elastic foundation indeed increases the natural frequency and this effect can be significant when the plate thickness is small but diminishes as the thickness becomes large.

4 Summary

A new non-classical Kirchhoff plate model is developed using a modified couple stress theory, a surface elasticity theory and a two-parameter elastic foundation model via a variational formulation based on Hamilton's principle. The equations of motion and the complete boundary conditions are determined simultaneously, and the microstructure, surface energy and foundation effects are treated in a unified manner. The new model contains a material length scale parameter to describe the microstructure effect, three surface elastic constants to account for the surface energy effect, and two foundation moduli to represent the foundation effect. The inclusion of the additional material constants enables the new model to capture the microstructure- and surface energy-dependent size effects.

It is shown that when the microstructure, surface energy, and foundation effects are all ignored, the new plate model recovers its classical elasticity-based counterpart as a limiting case. Also, it is seen that the newly developed plate model includes the models considering the microstructure dependence or the surface energy effect or the foundation effect alone as special cases and reduces to the Bernoulli–Euler beam model incorporating the microstructure, surface energy and foundation effects.

As direct applications of the new model, the static bending and free vibration problems of a simply supported rectangular plate are analytically solved, with the solutions compared to those based on the classical Kirchhoff plate theory. The numerical results show that the deflection of the simply supported plate with or without the elastic foundation predicted by the current model is smaller than that predicted by the classical model. Also, it is observed that the difference in the deflection predicted by the two plate models is very large when the plate thickness is sufficiently small, but it is diminishing with the increase of the plate thickness. In addition, it is found that the natural frequency predicted by the new plate model with or without the foundation is higher than that predicted by the classical plate model, and the difference is significant for very thin plates. These predicted size effects at the micron scale agree with the general trends observed in experiments (e.g., [19,32,55]). Finally, both the analytical formulas and the numerical results show that the plate deflection is reduced and the plate natural frequency is increased in the presence of the elastic foundation, as expected.

Acknowledgments The work reported here is funded by a grant from the U.S. National Science Foundation (NSF), Mechanics of Materials Program, with Dr. Thomas Siegmund as the program manager. This support is gratefully acknowledged. The author also would like to thank two anonymous reviewers for their encouragement and helpful comments on an earlier version of the paper.

References

1. Akgöz, B., Civalek, Ö.: Modeling and analysis of micro-sized plates resting on elastic medium using the modified couple stress theory. Meccanica **48**, 863–873 (2013)
2. Alessandroni, S., Andreaus, U., dell'Isola, F., Porfiri, M.: Piezo-electromechanical (PEM) Kirchhoff-Love plates. Eur. J. Mech. A/Solids. **23**, 689–702 (2004)
3. Altenbach, H., Eremeyev, V.A., Lebedev, L.P.: On the existence of solution in the linear elasticity with surface stresses. Z. Angew. Math. Mech. **90**, 231–240 (2010)
4. Cammarata, R.C.: Surface and interface stress effects in thin films. Prog. Surf. Sci. **46**, 1–38 (1994)
5. Eringen, A.C.: On differential equations of nonlocal elasticity and solutions of screw dislocation and surface waves. J. Appl. Phys. **54**, 4703–4710 (1983)
6. Eringen, A.C., Edelen, D.G.B.: On nonlocal elasticity. Int. J. Eng. Sci. **10**, 233–248 (1972)
7. Gao, X.-L.: A new Timoshenko beam model incorporating microstructure and surface energy effects. Acta Mech. **226**, 457–474 (2015)
8. Gao, X.-L., Huang, J.X., Reddy, J.N.: A non-classical third-order shear deformation plate model based on a modified couple stress theory. Acta Mech. **224**, 2699–2718 (2013)
9. Gao, X.-L., Ma, H.M.: Solution of Eshelby's inclusion problem with a bounded domain and Eshelby's tensor for a spherical inclusion in a finite spherical matrix based on a simplified strain gradient elasticity theory. J. Mech. Phys. Solids. **58**, 779–797 (2010)
10. Gao, X.-L., Mahmoud, F.F.: A new Bernoulli–Euler beam model incorporating microstructure and surface energy effects. Z. Angew. Math. Phys. **65**, 393–404 (2014)
11. Gao, X.-L., Mall, S.: Variational solution for a cracked mosaic model of woven fabric composites. Int. J. Solids Struct. **38**, 855–874 (2001)
12. Gao, X.-L., Park, S.K.: Variational formulation of a simplified strain gradient elasticity theory and its application to a pressurized thick-walled cylinder problem. Int. J. Solids Struct. **44**, 7486–7499 (2007)
13. Gao, X.-L., Zhang, G.Y.: A microstructure- and surface energy-dependent third-order shear deformation beam model. Z. Angew. Math. Phys. (published online on 13 Sept. 2014). doi:10.1007/s00033-014-0455-0
14. Gao, X.-L., Zhou, S.-S.: Strain gradient solutions of half-space and half-plane contact problems. Z. Angew. Math. Phys. **64**, 1363–1386 (2013)
15. Gurtin, M.E., Murdoch, A.I.: A continuum theory of elastic material surfaces. Arch. Ration. Mech. Anal. **57**, 291–323 (1975)
16. Gurtin, M.E., Murdoch, A.I.: Surface stress in solids. Int. J. Solids Struct. **14**, 431–440 (1978)
17. Jing, G.Y., Duan, H.L., Sun, X.M., Zhang, Z.S., Xu, J., Li, Y.D., Wang, J.X., Yu, D.P.: Surface effects on elastic properties of silver nanowires: contact atomic-force microscopy. Phy. Rev. B. **73**, 235409-1–235409-6 (2006)
18. Jomehzadeh, E., Noori, H.R., Saidi, A.R.: The size-dependent vibration analysis of micro-plates based on a modified couple stress theory. Phys. E. **43**, 877–883 (2011)
19. Lam, D.C.C., Yang, F., Chong, A.C.M., Wang, J., Tong, P.: Experiments and theory in strain gradient elasticity. J. Mech. Phys. Solids. **51**, 1477–1508 (2003)
20. Lazar, M., Maugin, G.A., Aifantis, E.C.: On a theory of nonlocal elasticity of bi-Helmholtz type and some applications. Int. J. Solids Struct. **43**, 1404–1421 (2006)
21. Lazopoulos, K.A.: On the gradient strain elasticity theory of plates. Euro. J. Mech. A/Solids. **23**, 843–852 (2004)
22. Lazopoulos, K.A.: On bending of strain gradient elastic micro-plates. Mech. Res. Commun. **36**, 777–783 (2009)
23. Lim, C.W., He, L.H.: Size-dependent nonlinear response of thin elastic films with nano-scale thickness. Int. J. Mech. Sci. **46**, 1715–1726 (2004)
24. Liu, C., Rajapakse, R.K.N.D.: Continuum models incorporating surface energy for static and dynamic response of nanoscale beams. IEEE Trans. Nanotech. **9**, 422–431 (2010)
25. Lu, P., He, L.H., Lee, H.P., Lu, C.: Thin plate theory including surface effects. Int. J. Solids Struct. **43**, 4631–4647 (2006)
26. Lu, P., Zhang, P.Q., Lee, H.P., Wang, C.M., Reddy, J.N.: Non-local elastic plate theories. Proc. R. Soc. A. **463**, 3225–3240 (2007)
27. Lü, C.F., Wu, D.Z., Chen, W.Q.: Nonlinear responses of nanoscale FGM films including the effects of surface energies. IEEE Trans. Nanotech. **10**, 1321–1327 (2011)
28. Ma, H.M., Gao, X.-L., Reddy, J.N.: A microstructure-dependent Timoshenko beam model based on a modified couple stress theory. J. Mech. Phys. Solids. **56**, 3379–3391 (2008)
29. Ma, H.M., Gao, X.-L., Reddy, J.N.: A non-classical Reddy-Levinson beam model based on a modified couple stress theory. Int. J. Multiscale Comput. Eng. **8**, 167–180 (2010)
30. Ma, H.M., Gao, X.-L., Reddy, J.N.: A non-classical Mindlin plate model based on a modified couple stress theory. Acta Mech. **220**, 217–235 (2011)
31. Maugin, G.A.: A historical perspective of generalized continuum mechanics. In: Altenbach, H., Maugin, G.A., Erofeev, V. (eds.) Mechanics of Generalized Continua., pp. 3–19. Springer, Berlin (2011)
32. McFarland, A.W., Colton, J.S.: Role of material microstructure in plate stiffness with relevance to microcantilever sensors. J. Micromech. Microeng. **15**, 1060–1067 (2005)
33. Miller, R.E., Shenoy, V.B.: Size-dependent elastic properties of nanosized structural elements. Nanotech. **11**, 139–147 (2000)
34. Mindlin, R.D.: Influence of couple-stresses on stress concentrations. Exp. Mech. **3**, 1–7 (1963)

35. Mindlin, R.D.: Micro-structure in linear elasticity. Arch. Ration. Mech. Anal. **16**, 51–78 (1964)
36. Papargyri-Beskou, S., Beskos, D.E.: Static, stability and dynamic analysis of gradient elastic flexural Kirchhoff plates. Arch. Appl. Mech. **78**, 625–635 (2008)
37. Papargyri-Beskou, S., Giannakopoulos, A.E., Beskos, D.E.: Variational analysis of gradient elastic flexural plates under static loading. Int. J. Solids Struct. **47**, 2755–2766 (2010)
38. Park, S.K., Gao, X.-L.: Bernoulli–Euler beam model based on a modified couple stress theory. J. Micromech. Microeng. **16**, 2355–2359 (2006)
39. Park, S.K., Gao, X.-L.: Variational formulation of a modified couple stress theory and its application to a simple shear problem. Z. Angew. Math. Phys. **59**, 904–917 (2008)
40. Placidi, L., Rosi, G., Giorgio, I., Madeo, A.: Reflection and transmission of plane waves at surfaces carrying material properties and embedded in second gradient materials. Math. Mech. Solids. **19**, 555–578 (2014)
41. Reddy, J.N.: Energy Principles and Variational Methods in Applied Mechanics, 2nd edn. Wiley, Hoboken, New Jersey (2002)
42. Ru, C.Q.: Simple geometrical explanation of Gurtin–Murdoch model of surface elasticity with clarification of its related versions. Sci. China Phys. Mech. Astron. **53**, 536–544 (2010)
43. Selvadurai, A.P.S.: Elastic Analysis of Soil-Foundation Interaction. Elsevier, Amsterdam (1979)
44. Shaat, M., Mahmoud, F.F., Gao, X.-L., Faheem, A.F.: Size-dependent bending analysis of Kirchhoff nano-plates based on a modified couple-stress theory including surface effects. Int. J. Mech. Sci. **79**, 31–37 (2014)
45. Shenoy, V.B.: Atomistic calculations of elastic properties of metallic fcc crystal surfaces. Phys. Rev. B. **71**, 094104-1–094104-11 (2005)
46. Steigmann, D.J.: The variational structure of a nonlinear theory for spatial lattices. Meccanica **31**, 441–455 (1996)
47. Steigmann, D.J.: Thin-plate theory for large elastic deformations. Int. J. Non-Linear Mech. **42**, 233–240 (2007)
48. Steigmann, D.J., Ogden, R.W.: Plane deformations of elastic solids with intrinsic boundary elasticity. Proc. R. Soc. Lond. A. **453**, 853–877 (1997)
49. Steigmann, D.J., Ogden, R.W.: Elastic surface-substrate interactions. Proc. R. Soc. Lond. A. **455**, 437–474 (1999)
50. Timoshenko, S.P., Goodier, J.N.: Theory of Elasticity, 3rd edn. McGraw-Hill, New York (1970)
51. Tsiatas, G.C.: A new Kirchhoff plate model based on a modified couple stress theory. Int. J. Solids Struct. **46**, 2757–2764 (2009)
52. Wang, K.F., Wang, B.L.: Effects of residual surface stress and surface elasticity on the nonlinear free vibration of nanoscale plates. J. Appl. Phys. **112**, 013520-1–013520-6 (2012)
53. Yang, F., Chong, A.C.M., Lam, D.C.C., Tong, P.: Couple stress based strain gradient theory for elasticity. Int. J. Solids Struct. **39**, 2731–2743 (2002)
54. Yokoyama, T.: Vibration analysis of Timoshenko beam-columns on two-parameter elastic foundations. Comput. Struct. **61**, 995–1007 (1996)
55. Zhang, Y., Zhuo, L.J., Zhao, H.S.: Determining the effects of surface elasticity and surface stress by measuring the shifts of resonant frequencies. Proc. R. Soc. A. **469**, 20130449-1–20130449-14 (2013)
56. Zhou, S.-S., Gao, X.-L.: Solutions of half-space and half-plane contact problems based on surface elasticity. Z. Angew. Math. Phys. **64**, 145–166 (2013)
57. Zhou, S.-S., Gao, X.-L.: A non-classical model for circular Mindlin plates based on a modified couple stress theory. ASME J. Appl. Mech. **81**, 051014-1–051014-8 (2014)
58. Zhou, S.-S., Gao, X.-L.: Solutions of the generalized half-plane and half-space Cerruti problems with surface effects. Z. Angew. Math. Phys. (published online on 16 April 2014). doi:10.1007/s00033-014-0419-4